

# Monte-Carlo studies of multiple-fibre reconstruction algorithms for diffusion MRI

D. C. Alexander<sup>1</sup>

<sup>1</sup>Computer Science, UCL (University College London), London, United Kingdom

**Introduction** This abstract uses Monte-Carlo simulations to compare the precision and accuracy of reconstructed fibre directions from three recent diffusion-MRI reconstruction algorithms: PASMRI [1], Qball [2] and spherical deconvolution [3]. We limit investigation to a spherical sampling scheme and use simple test functions for the particle-displacement density function  $p$ . This extends preliminary work in [4], which compares the fraction of trials in which PASMRI and Qball recover approximately the right direction from similar test functions with no false positive directions. The results in [4] show that PASMRI recovers directions more consistently at lower SNR and  $b$ -values than Qball.

**Methods** All three algorithms return a function of the sphere with peaks that provide fibre-orientation estimates. In PASMRI, the function is called the persistent angular structure (PAS). In Qball, the function is an approximation to the orientation distribution function (ODF). In spherical deconvolution, the recovered function is called the fibre-orientation distribution (FOD).

We use variations of three simple test functions:  $p_1 = G(\mathbf{x}; D_1, t)$  (one-fibre simulation),  $p_3 = \alpha G(\mathbf{x}; D_1, t) + (1 - \alpha) G(\mathbf{x}; D_2, t)$  (two-fibre simulation) and  $p_4 = (G(\mathbf{x}; D_1, t) + G(\mathbf{x}; D_2, t) + G(\mathbf{x}; D_3, t))/3$  (three-fibre simulation), where  $\alpha \in [0, 1]$  is a mixing parameter,  $G(\bullet; D, t)$  is the zero-mean Gaussian function with covariance  $2tD$  and the diffusion tensors are  $D_1 = \text{diag}(\lambda_1, \lambda_2, \lambda_2)$ ,  $D_2 = \text{diag}(\lambda_2, \lambda_1, \lambda_2)$  and  $D_3 = \text{diag}(\lambda_2, \lambda_2, \lambda_1)$ . By default,  $\alpha = 0.5$ ,  $\lambda_1 = 1.7 \times 10^{-9} \text{ m}^2 \text{ s}^{-1}$  and  $\text{Tr}(D_i) = \lambda_1 + 2\lambda_2 = 2.1 \times 10^{-9} \text{ m}^2 \text{ s}^{-1}$ . We synthesize data by sampling the Fourier transform  $F$  of  $p$  at each wavenumber sampled by the imaging sequence, adding a random complex number with independent real and imaginary parts drawn from  $N(0, \sigma^2)$ , where  $\sigma = F(0)/S$  and  $S$  is the signal to noise ratio at  $b = 0$ , and taking the modulus.

We determine the peak directions of the PAS, ODF and FOD numerically. In each case, we sample the function at each vertex of 1000 random rotations of a regular icosahedron. We find the list of sampled points that are local maxima in the sense that the function is larger at that point than any other sampled location within a search radius, which we set to 0.4, of that point. Finally, we refine the locations of the peaks from these local maxima using Powell's local optimisation algorithm [5].

To determine the precision and accuracy of recovered orientations, we run 256 independent trials. We use a simple clustering technique to associate corresponding peaks between different trials. To compute the concentration of a population of corresponding directions, we compute the mean dyadic tensor  $Y = \sum_i \mathbf{x}_i \mathbf{x}_i^T$  and take the largest eigenvalue  $\kappa_1$ , which is zero for isotropically distributed directions and one for a population of equal directions. The corresponding eigenvector  $\mu_1$  is the mean direction of the population. We repeat this experiment over 10 random rotations of the test function and compute the mean, maximum and minimum  $\kappa_1$ . For a better comparison scale, we use  $\chi(\kappa_1) = -\log(1 - \kappa_1)$  as the direction-concentration statistic. A distribution of directions with 95% of the samples within  $60^\circ$  of the mean has  $\chi(\kappa_1) \approx 2$ ; when the 95 percentile is  $10^\circ$  from the mean,  $\chi(\kappa_1) \approx 5$ , and when it is  $3^\circ$  from the mean,  $\chi(\kappa_1) \approx 7$ . For Qball and PASMRI, we use the parameter settings specified in [4], which crudely maximize the number of trials that give the expected number of peak directions. For spherical deconvolution, we use the default parameter settings of the software [3].

**Experiments and Results** Figure 1 plots the mean (over the 10 rotations)  $\kappa_1$  of the most significant (on average) peak direction as a function of non-zero  $b$ -value in the spherical sampling scheme for  $p_1$ ,  $p_3$  and  $p_4$  using PASMRI, Qball and spherical deconvolution. The error bars show the maximum and minimum  $\kappa_1$  over the 10 rotations. The spherical sampling scheme has six measurements at  $b = 0$  and 54 measurements at the non-zero  $b$ , which come from the electrostatic energy minimization in [1]. We model a PGSE sequence with EPI readout on a standard 1.5T scanner to estimate the TE required for each  $b$ -value and reduce the signal to noise ratio,  $S$ , accordingly assuming  $T_2 = 0.08 \text{ s}$ . We take  $S=20$  when  $b = 1.0 \times 10^9 \text{ s m}^{-2}$ .

Additional experiments study the precision and accuracy of the reconstructions as the angle  $(\pi/2 - a)$  between the principal directions in  $p_3$  changes. In this experiment, we mimic the parameters of an imaging sequence that is in routine use at an imaging centre in London. This sequence also acquires 6 measurements at  $b = 0$  and acquires 54 measurements with  $b = 1.6 \times 10^9 \text{ s m}^{-2}$ . We take  $S=16$ , which is close to that observed in scanner data in white matter regions. Figure 2 shows the bias in one of the reconstructed direction by plotting the average (over the 10 rotations) angle between  $\mu_1$  and the closest principal direction of the test function. The plot for the second direction shows similar trends.

**Conclusions and Further Work** The results show that the optimal  $b$ -values for the methods differ for these test function. Qball and PASMRI are best with  $b \in [1.0, 1.5] \times 10^9 \text{ s m}^{-2}$  in the one-fibre case and  $b \approx 2.0 \times 10^9 \text{ s m}^{-2}$  for two or three fibres. Spherical deconvolution requires much higher  $b$ -values in the one-fibre case and slightly higher for two or three fibres. The peak direction-concentrations are similar for Qball and PASMRI, but lower for spherical deconvolution. Note that  $\kappa_1$  is insensitive to spurious or missing peaks, so the results shown here should be considered in parallel to those in [4]. The results of varying  $a$  show that PASMRI gives the lowest bias; the large error bars for Qball and spherical deconvolution suggest that these algorithms fail at this low SNR and  $b$ -value. Further simulations will characterize the relative performance of these algorithms in more detail.

## References

1. Jansons, K.M. and Alexander, D.C., *Inverse Problems*, 19, 1031, 2003.
2. Tuch, D.S., *et al*, *Neuron*, 40, 885, 2003.
3. Tournier, J. D, *et al*, *NeuroImage*, 23, 1176, 2004.
4. Alexander, D.C., *Proc. ISMRM*, 90, 2004.
5. Press, W.H., *et al*, *Numerical Recipes in C*, CUP, 1988.

**Acknowledgements** DCA is funded by the MIAS IRC: EPSRC GR/N14248/01, MRC D2025/31; and EPSRC: GR/T22858/01. The author thanks Dave Tuch for his Qball code and Donald Tournier for his spherical deconvolution code.

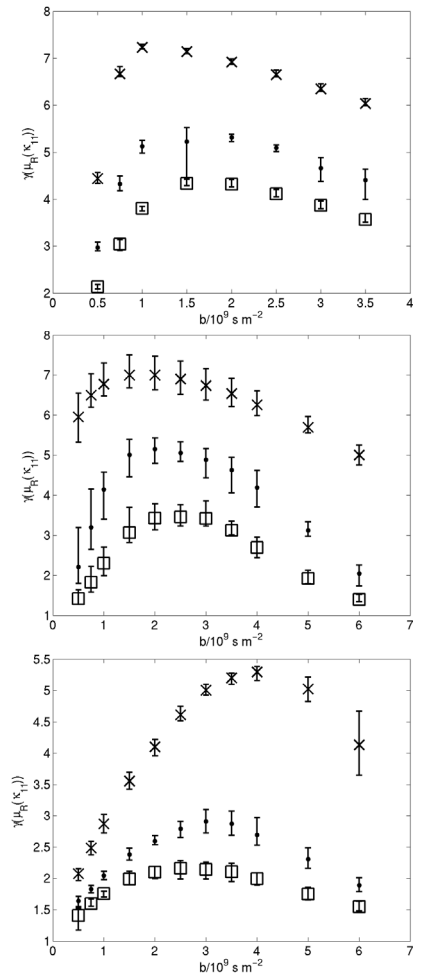


Figure 1. Average  $\kappa_1$  of one reconstructed direction from  $p_1$  ( $\times$ ),  $p_3$  ( $\bullet$ ) and  $p_4$  ( $\square$ ) with PASMRI (top), Qball (centre) and deconvolution (bottom) against  $b$ .

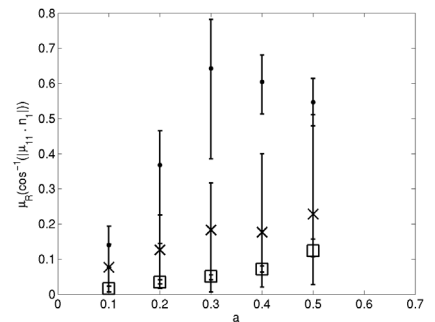


Figure 2. Shows the average bias in reconstructed directions for spherical deconvolution ( $\times$ ), Qball ( $\bullet$ ) and PASMRI ( $\square$ ) as the angle between the true directions  $(\pi/2 - a)$  varies